

## Supporting Information

### The effect of photocatalyst excited state lifetime on the rate of photoredox catalysis

J. R. Ochola and M. O. Wolf\*

---

*Department of Chemistry, University of British Columbia, 2036 Main Mall, Vancouver, British Columbia, V6T 1Z1, Canada.*

#### Table of Contents

1.	General information	2
2.	Preparation of iridium(III) polypyridyl complexes	2
3.	General procedure for photoredox-catalyzed trifluoromethylation of quinoline	2
4.	Stern-Volmer experiments	5
5.	Absorption spectra of photocatalysts	6
6.	Emission spectra of photocatalysts ( $E_{0,0}$ determination)	7
7.	Emission lifetime measurements of photocatalysts	8
8.	Cyclic voltammograms of photocatalysts	9
9.	Calculation of $\Delta G_{ET}^{\circ}$	10
10.	Electrochemical experiments of <b>2</b> with quinoline	11
11.	Photoredox catalysis varying $\text{CF}_3\text{SO}_2\text{Cl}$ concentration	12
12.	NMR Spectra	13
13.	References	20

## 1. General information

$^1\text{H}$  NMR and  $^{19}\text{F}$  NMR spectra were recorded on a Bruker AV-400 spectrometer and referenced to the residual protonated solvent peak. Electrospray ionization (ESI) mass spectra (MS) were obtained on a Bruker Esquire LC ion trap mass spectrometer. Microwave reactions were performed using a Biotage Initiator 2.5 microwave synthesizer. Absorption spectra were obtained on a Varian Cary 5000 UV-vis-near-IR spectrophotometer. Fluorescence spectra were collected on a Photon Technology International QuantaMaster fluorimeter. Gas chromatography-mass spectrometry (GC-MS) was carried out using an Agilent Technologies 7890B GC system equipped with a 5977A MS detector and 7693 autosampler.

**Materials.** All reagents were used as purchased from commercial sources. HPLC grade acetonitrile was used and deuterated solvents used for NMR analysis were purchased from Sigma-Aldrich.

## 2. Preparation of iridium(III) polypyridyl complexes

$[\text{Ir}(\text{ppy})_2\text{Cl}]_2$  (0.070 g, 0.065 mmol),  $\text{KPF}_6$  (0.0242 g, 0.131 mmol), and the appropriate bipyridine ligand (0.0145 mmol) were placed in a microwave vial equipped with a magnetic stir bar. Ethanol (3.6 mL) was added to the vial and the suspension was degassed for 10 minutes using nitrogen gas, after which time the reaction vial was placed in the microwave reactor and heated with microwave irradiation for 30 minutes at 100 °C (18 bar, 155 W). The work-up and purification procedures, as well as the synthesis of the dimer  $[\text{Ir}(\text{ppy})_2\text{Cl}]_2$  were similar to those previously reported by Wolf *et al.*<sup>1</sup>

$[\text{Ir}(\text{ppy})_2\text{phen}][\text{PF}_6]$  (**1**):  $^1\text{H}$  NMR ( $\text{CD}_3\text{CN}$ , 300 MHz):  $\delta$  8.68 (2H, dd,  $J = 8.2, 1.3$  Hz), 8.30 (2H, dd,  $J = 5.1, 1.3$  Hz), 8.23 (2H, s), 8.05 (2H, d,  $J = 8.5$  Hz), 7.87-7.75 (6H, m), 7.43-7.41 (2H, m), 7.09 (2H, td,  $J = 7.5, 7.5, 1.2$  Hz), 6.97 (2H, td,  $J = 7.6, 7.6, 1.3$  Hz), 6.85 (2H, ddd,  $J = 7.4, 6, 1.3$  Hz), 6.39 ppm (2H, dd,  $J = 7.3, 0.9$  Hz). MS ( $m/z$ ; ESI): 681 (100%,  $\text{M} - \text{PF}_6 + \text{H}^+$ ). The characterization data matches that found in the literature.<sup>2(a)</sup>

$[\text{Ir}(\text{ppy})_2\text{dtbbpy}][\text{PF}_6]$  (**2**):  $^1\text{H}$  NMR ( $\text{CD}_3\text{CN}$ , 300 MHz):  $\delta$  8.48 (2H, d,  $J = 1.8$  Hz), 8.05 (2H, d,  $J = 8.2$  Hz), 7.86-7.77 (6H, m), 7.59-7.57 (2H, m), 7.49 (2H, dd,  $J = 5.9, 1.8$  Hz), 7.06-7.00 (4H, m), 6.90 (2H, td,  $J = 7.4, 7.4, 1.3$  Hz), 6.27 (2H, dd,  $J = 7.1, 0.6$  Hz), 1.4 ppm (18H, s). MS ( $m/z$ ; ESI): 770 (100%,  $\text{M} - \text{PF}_6 + \text{H}^+$ ). The characterization data matches that found in the literature.<sup>2(b)</sup>

$[\text{Ir}(\text{ppy})_2\text{dmbpy}][\text{PF}_6]$  (**3**):  $^1\text{H}$  NMR ( $\text{CD}_3\text{CN}$ , 300 MHz):  $\delta$  8.37 (2H, s), 8.07-8.04 (2H, m), 7.86-7.77 (6H, m), 7.61-7.59 (2H, m), 7.32-7.30 (2H, m), 7.06-7.00 (4H, m), 6.90 (2H, td,  $J = 7.4, 7.4, 1.3$  Hz), 6.28 (2H, dd,  $J = 7.6, 1.2$  Hz), 2.50 ppm (6H, s). MS ( $m/z$ ; ESI): 685 (100%,  $\text{M} - \text{PF}_6 + \text{H}^+$ ). The characterization data matches that found in the literature.<sup>2(c)</sup>

$[\text{Ir}(\text{ppy})_2\text{bpy}][\text{PF}_6]$  (**4**):  $^1\text{H}$  NMR ( $\text{CD}_3\text{CN}$ , 300 MHz):  $\delta$  8.52 (2H, d,  $J = 7.9$  Hz), 8.12 (2H, td,  $J = 7.9, 7.9, 1.8$  Hz), 8.06 (2H, d,  $J = 8.2$  Hz), 7.99-7.97 (2H, m), 7.87-7.79 (4H, m), 7.60 (2H, dt,  $J = 5.8, 0.7, 0.7$  Hz), 7.50 (2H, ddd,  $J = 7.6, 5.5, 1.0$  Hz), 7.07-7.00 (4H, m), 6.92 (2H, td,  $J = 7.4, 7.4, 1.4$  Hz), 6.28 ppm (2H, dd,  $J = 7.6, 0.6$  Hz). MS ( $m/z$ ; ESI): 657 (100%,  $\text{M} - \text{PF}_6 + \text{H}^+$ ). The characterization data matches that found in the literature.<sup>2(d)</sup>

## 3. General procedure for photoredox-catalyzed trifluoromethylation of quinoline

The procedure used was a modified version of that reported by MacMillan *et al.*<sup>3</sup> The appropriate iridium complex (0.005 mmol) and  $\text{K}_2\text{HPO}_4$  (0.261 g, 1.5 mmol, 3 equiv.) were placed in a 20 mL scintillation vial equipped with a magnetic stir bar. Acetonitrile (4 mL) was transferred to the vial and the vial sealed with a septum. The suspension was degassed with vigorous stirring for 10 minutes using nitrogen gas. Quinoline (60  $\mu\text{L}$ , 0.5 mmol for a 0.12 M solution and 300  $\mu\text{L}$ , 2.5 mmol for a 0.60 M solution), cyclohexane carbonitrile internal standard (40  $\mu\text{L}$ , 0.3 mmol) and  $\text{CF}_3\text{SO}_2\text{Cl}$  (0.1 mL, 0.9 mmol, 1.8 equiv.) were injected into the vial using a syringe. The reaction vessel was then irradiated using a 13W “daylight” compact fluorescent bulb and 0.1 mL aliquots were removed at various time intervals and diluted to 10 mL in a volumetric flask before analysis by GC-MS. Photocatalysts **2** and **4** were used to follow the trifluoromethylation of quinoline at 0.12 M and 0.60 M initial quinoline concentrations (the concentrations of all reagents other than quinoline were kept constant). The quantification of product was accomplished by dividing the total integrated area for all product peaks (P) by the total integrated area of the internal standard (S) to give the ratio P/S that allowed for the comparison of product formation across reactions with the same amount of

internal standard. The crude mixture was purified by preparative thin-layer chromatography, after which the products were characterized by  $^1\text{H}$  and  $^{19}\text{F}$  NMR. The characterization data for the products generally match that found in the literature.<sup>4</sup>

5-trifluoromethylquinoline:  $^1\text{H}$  NMR ( $\text{CDCl}_3$ , 300 MHz):  $\delta$  9.03 (1H, d,  $J$  = 3.6 Hz), 8.56 (1H, d,  $J$  = 9.2 Hz), 8.36 (1H, d,  $J$  = 8.5 Hz), 7.97 (1H, d,  $J$  = 7.4 Hz), 7.82-7.76 (1H, m), 7.57 ppm (1H, dd,  $J$  = 8.7, 4.4 Hz).  $^{19}\text{F}$  NMR ( $\text{CDCl}_3$ , 300 MHz):  $\delta$  -59.44 ppm.<sup>4(a)</sup> MS ( $m/z$ ): 197 (100%,  $\text{M}^+$ ).

8-trifluoromethylquinoline:  $^1\text{H}$  NMR ( $\text{CDCl}_3$ , 300 MHz):  $\delta$  9.11 (1H, dd,  $J$  = 4.1, 1.8 Hz), 8.25 (1H, dd,  $J$  = 8.5, 1.8 Hz), 8.11 (1H, d,  $J$  = 7.2 Hz), 8.04 (1H, d,  $J$  = 8.5 Hz), 7.62 (1H, t,  $J$  = 7.8 Hz), 7.54 ppm (1H, dd,  $J$  = 8.3, 4.2 Hz).  $^{19}\text{F}$  NMR ( $\text{CDCl}_3$ , 300 MHz):  $\delta$  -60.57 ppm.<sup>4(b)</sup> MS ( $m/z$ ): 197 (100%,  $\text{M}^+$ ).

5,8-di(trifluoromethyl)quinoline:  $^1\text{H}$  NMR ( $\text{CDCl}_3$ , 300 MHz):  $\delta$  9.18 (1H, dd,  $J$  = 4.2, 1.7 Hz), 8.59 (1H, dt,  $J$  = 8.7, 1.8, 1.8 Hz), 8.16 (1H, d,  $J$  = 7.7 Hz), 8.01 (1H, d,  $J$  = 7.9 Hz), 7.67 ppm (1H, dd,  $J$  = 8.7, 4.1 Hz).  $^{19}\text{F}$  NMR ( $\text{CDCl}_3$ , 300 MHz):  $\delta$  -59.96, -61.06 ppm. MS ( $m/z$ ): 215 (100%,  $\text{M}^+$ ).

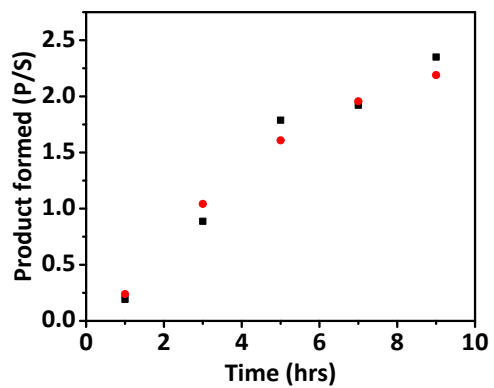


**Fig. S1** Formation of trifluoromethylated quinoline over time using **2** (black squares) and **4** (red circles) at 0.12 M quinoline concentration.

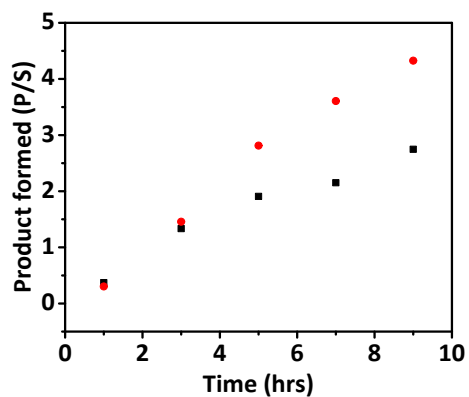


**Fig. S2** Formation of trifluoromethylated quinoline over time using **2** at 0.12 M quinoline (black squares) and 0.60 M quinoline (red circles) concentration.

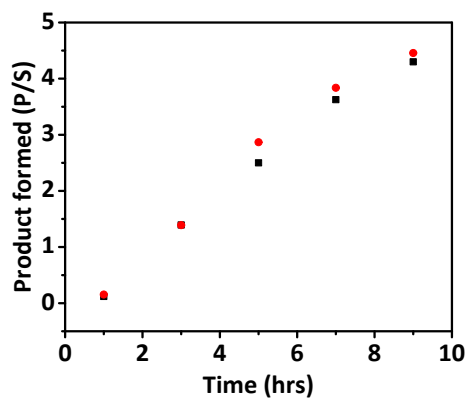


**Fig. S3** Formation of trifluoromethylated quinoline over time using **2** (black squares) and **4** (red circles) at 0.60 M quinoline concentration.

#### 4. Stern-Volmer experiments

Stock solutions of each of the iridium complexes in acetonitrile ( $10^{-3}$  M) were made by dissolving 0.01 mmol of the complex in 10 mL of acetonitrile. Aliquots (0.1 mL) of the stock iridium solutions were added to 10 mL volumetric flasks with the appropriate amount of  $\text{CF}_3\text{SO}_2\text{Cl}$  stock solution (made by topping up 0.1 mL of pure  $\text{CF}_3\text{SO}_2\text{Cl}$  to 10 mL using acetonitrile in a volumetric flask) and diluted to 10 mL using acetonitrile. All solutions were degassed for 15 minutes using argon gas before the steady-state emission spectra were obtained. The quenching of photocatalyst **2** emission by  $\text{CF}_3\text{SO}_2\text{Cl}$  was measured as a control alongside the emission quenching experiments for the other three photocatalysts to take into account changes in temperature and moisture that may affect the quenching efficiency and reactivity. The average  $K_{SV}$  value for **2**,  $K_{SV,contr,avg}$ , was determined from three replicate quenching experiments (Fig. S4) and used to correct the  $K_{SV}$  values of the other photocatalysts,  $K_{SV,exp}$ , using eqn S1 to give  $K_{SV,corr}$  for each experiment ( $K_{SV,contr,exp}$  is the unmodified  $K_{SV}$  value for the control experiment). The quenching experiments were run three times for each photocatalyst (see Fig. S5 for examples for each catalyst) and the reported  $K_{SV}$  value is an average of the three  $K_{SV,corr}$  values obtained.

$$K_{SV,corr} = \frac{(K_{SV,exp})(K_{SV,contr,avg})}{K_{SV,contr,exp}} \quad (\text{S1})$$

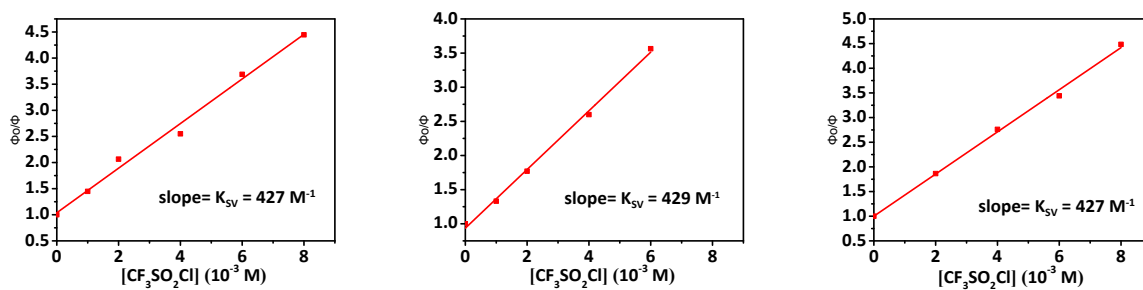


Fig. S4 Triplicate Stern-Volmer experiments for **2** with  $\text{CF}_3\text{SO}_2\text{Cl}$  as quencher.

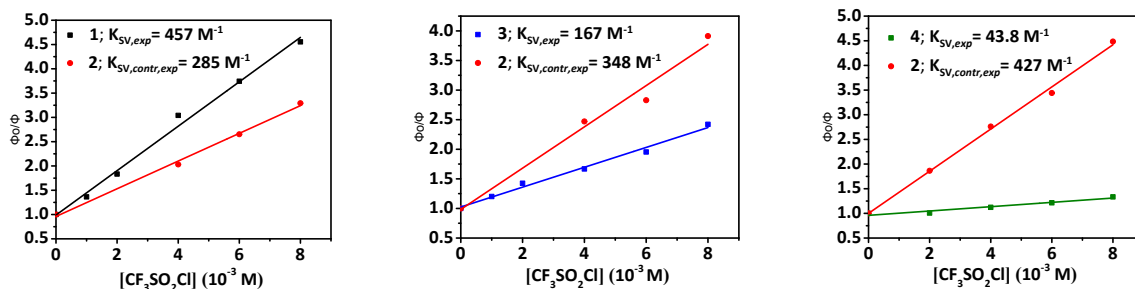
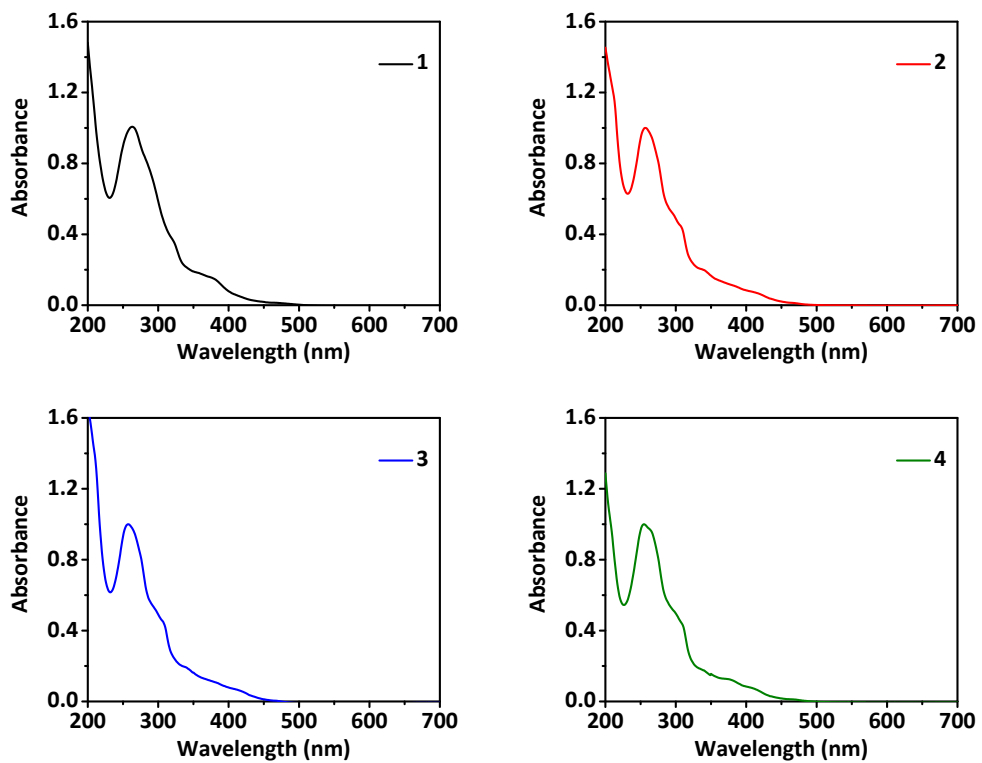


Fig. S5 Stern-Volmer analyses of photocatalysts **1,3** and **4** with that of **2** as a control.

## 5. Absorption spectra of photocatalysts



**Fig. S6** Absorption spectra of photocatalysts 1-4 ( $10^{-5}$  M solutions in acetonitrile).

## 6. Emission spectra of photocatalysts (and $E_{0,0}$ determination)

The emission profiles of the photocatalysts ( $10^{-5}$  M solutions in acetonitrile) were obtained after degassing for 15 minutes using argon gas. The spectra were plotted, and for each complex, the blue onset of emission was estimated and reported as  $E_{0,0}$ .

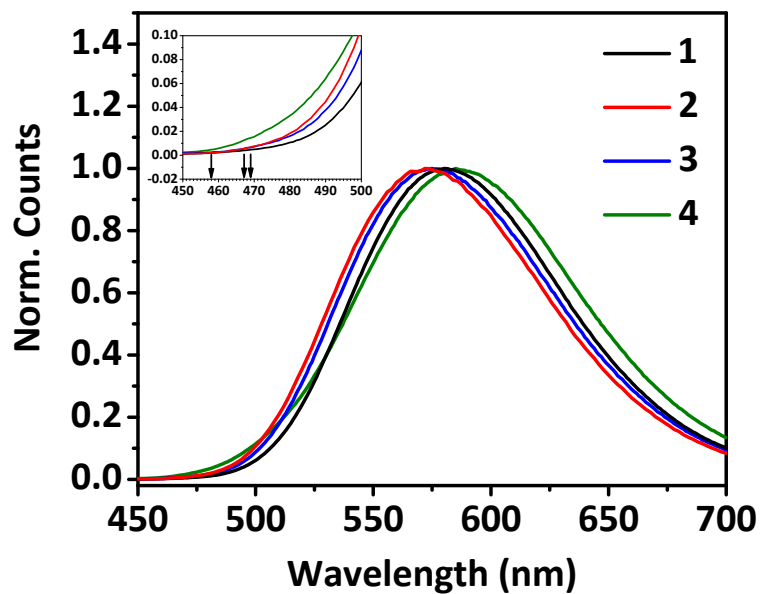


**Fig. S7** Emission spectra of photocatalysts 1-4 ( $10^{-5}$  M solutions in acetonitrile).

## 7. Emission lifetime measurements of photocatalysts

Solutions of the iridium complexes were made in acetonitrile ( $10^{-5}$  M) and degassed for 30 minutes before lifetime measurements were obtained.

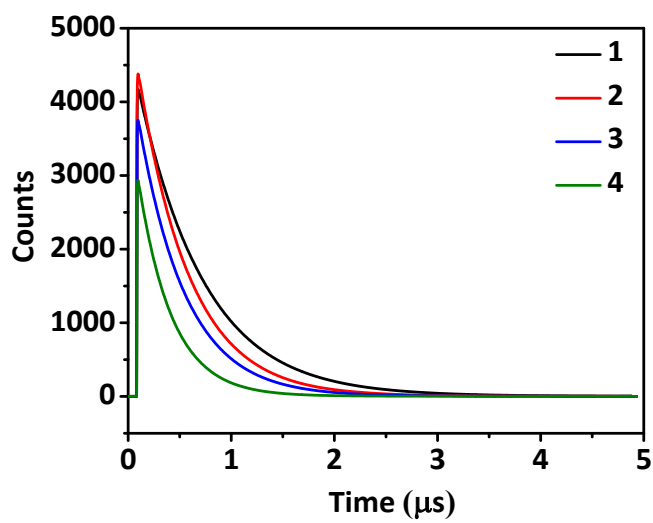


**Fig. S8** Emission lifetime measurements of photocatalysts 1-4 ( $10^{-5}$  M solutions in acetonitrile) fitted to single-exponential decay.



## 8. Cyclic voltammograms (CV) of photocatalysts

Dry acetonitrile (5 mL) was transferred to an electrochemical cell containing tetrabutylammonium tetrafluoroborate,  $[n\text{-Bu}_4\text{N}]\text{BF}_4$ , (0.164 g, 0.5 mmol) and the solution was degassed for 15 minutes using nitrogen gas. The CV profiles of these solutions were obtained as “blanks”. Then the photocatalyst (0.005 mmol, 1mM) was dissolved in the  $[n\text{-Bu}_4\text{N}]\text{BF}_4$  solution and the solution was degassed for an additional 5 minutes before the CV measurements were taken, after which time a few crystals of ferrocene (as an internal reference) were added and the solution degassed again for 5 minutes before the CV scan was taken with the reference present. Platinum wire was used as the working electrode, platinum mesh as the counter electrode and silver/silver oxide wire as the reference electrode. A potential sweep rate of 100 mV/s was used.

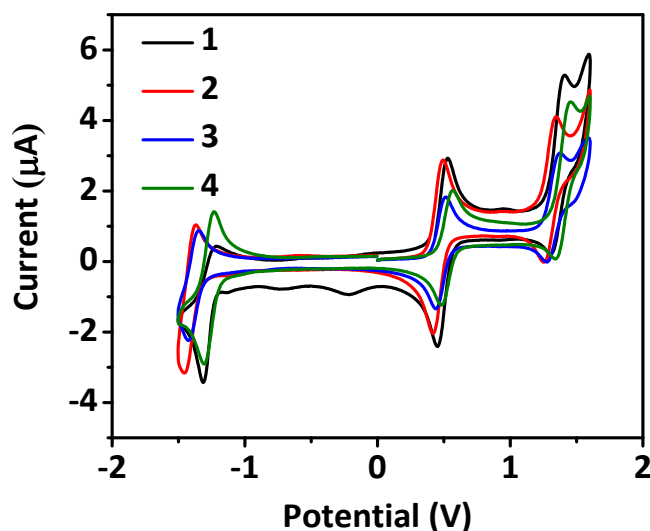


**Fig. S9** Cyclic voltammograms of photocatalysts 1-4 (1 mM solutions in acetonitrile) referenced to ferrocene.

**Table S1.** Thermodynamic properties of 1-4 associated with SET with  $\text{CF}_3\text{SO}_2\text{Cl}$ .

Entry	Photocatalyst	$E_{ox}^a$ (V)	$E_{0,0}^b$ (eV)	$r_{DC}$ (Å)	$a^d$ (Å)	$w(D^+ A^-)^e$ (eV)	$\Delta G_{ET}^f$ (eV)
1	$[\text{Ir}(\text{ppy})_2\text{phen}]\text{PF}_6$	+1.25	2.71	7.24	10.32	-0.0744	-1.35
2	$[\text{Ir}(\text{ppy})_2\text{dtbbpy}]\text{PF}_6$	+1.22	2.66	9.20	12.28	-0.0624	-1.32
3	$[\text{Ir}(\text{ppy})_2\text{dmbpy}]\text{PF}_6$	+1.23	2.64	7.83	10.91	-0.0702	-1.30
4	$[\text{Ir}(\text{ppy})_2\text{bpy}]\text{PF}_6$	+1.25	2.66	6.83	9.91	-0.0773	-1.31

<sup>a</sup> Values obtained by cyclic voltammetry in  $\text{CH}_3\text{CN}/[n\text{-Bu}_4\text{N}]\text{BF}_4$ ; values versus SCE and internally referenced to ferrocene.<sup>b</sup> Energy between zeroth vibrational state of the emissive excited and ground state, estimated as the energy at the blue onset of emission spectra of photocatalysts.<sup>c</sup> Electron donor radius; estimated as the distance from iridium to the furthest end of the largest ligand, obtained from crystal structures in the Cambridge Crystallographic Database.<sup>d</sup> Distance between the photocatalyst and  $\text{CF}_3\text{SO}_2\text{Cl}$  during SET, estimated as the sum of the radii of the photocatalyst and  $\text{CF}_3\text{SO}_2\text{Cl}$ .<sup>e</sup> Electrostatic work term associated with the effect of Coulombic attraction between products; see equation below.<sup>f</sup> Gibbs free energy change for the SET involving the excited photocatalyst and  $\text{CF}_3\text{SO}_2\text{Cl}$ ; see equation below.<sup>5</sup>

## 9. Calculation of $\Delta G_{ET}^\circ$

$$\Delta G_{ET}^\circ = e[E_{ox,D} - E_{red,A}] + w(D^{+} A^{-}) - w(DA) - E_{0,0}$$

$$w(D^{+} A^{-}) = \frac{Z_{D^{+}} Z_{A^{-}} e^2}{4\pi\epsilon_0\epsilon_r a}$$

$$w(DA) = \frac{Z_D Z_A e^2}{4\pi\epsilon_0\epsilon_r a}$$

$Z_D$	Charge of donor (photocatalyst) before SET	+1 for <b>1-4</b>
$Z_A$	Charge of acceptor (CF <sub>3</sub> SO <sub>2</sub> Cl) before SET	0
$Z_{D^{+}}$	Charge of donor after SET	+2 for <b>1-4</b>
$Z_{A^{-}}$	Charge of acceptor after SET	-1
$e$	Elementary charge	$1.60 \times 10^{-19}$ C
$\epsilon_0$	Electric constant OR vacuum permittivity	$8.85 \times 10^{-12}$ C <sup>2</sup> J <sup>-1</sup> m <sup>-1</sup>
$\epsilon_r$	Dielectric constant OR relative medium static permittivity	37.5 for acetonitrile
$a$	Sum of radii of acceptor and donor, $r_A + r_D$	See Table S1
$r_A$	Radius of acceptor	3.08 Å
$w(DA)$	Electrostatic work associated with bringing together reactants of SET	0, as $Z_A = 0$
$w(D^{+} A^{-})$	Electrostatic work associated with separating products of SET	See Table S1
$E_{0,0}$	Energy difference between zeroth vibrational energy states in ground and excited states of the photocatalyst	See Table S1
$E_{red,A}$	Reduction potential of acceptor	-0.18 V <sup>3</sup>
$E_{ox,D}$	Oxidation potential of donor	See Table S1

## 10. Electrochemical experiments of **2** with quinoline

Dry acetonitrile (10 mL) was transferred to an electrochemical cell containing  $[n\text{-Bu}_4\text{N}]\text{BF}_4$ , (0.360 g, 1.1 mmol, 0.1 M) and the colourless solution was degassed for 15 minutes using nitrogen gas. The CV profiles of these solutions were obtained as “blanks”. Then **2** (0.018 g, 0.020 mmol, 2.0 mM) was dissolved in the  $[n\text{-Bu}_4\text{N}]\text{BF}_4$  solution after which the solution was degassed for an additional 5 minutes before the CV measurements were taken. After the CV profile of the photocatalyst solution was obtained, quinoline (18  $\mu\text{L}$ , 0.15 mmol, 15 mM) was injected into the cell. The solution was degassed for an additional 5 minutes and the CV profile measured. Afterwards, the concentration of quinoline was doubled (addition of another 18  $\mu\text{L}$ ) after which the solution was degassed for 5 minutes and CV profile obtained (Fig. S10).

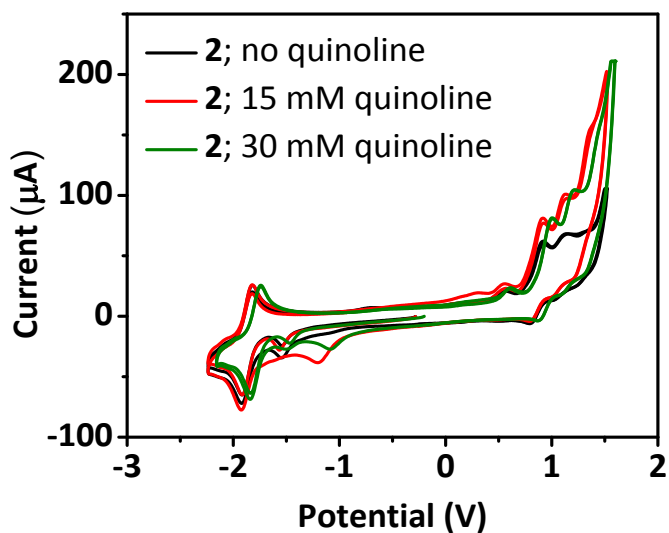


**Fig. S10** Cyclic voltammety profiles of **2** (2 mM) in acetonitrile at 0 mM (blue), 15 mM (red) and 30 mM (green) concentrations of quinoline.

## 11. Reaction rate dependence of $\text{CF}_3\text{SO}_2\text{Cl}$ concentration

The general procedure for the photoredox catalysis was followed using 0.1 mL (0.22 M) and 0.5 mL (1.10 M)  $\text{CF}_3\text{SO}_2\text{Cl}$ . The reaction rates were compared using photocatalyst **1** as well as **4** (Fig. S11).

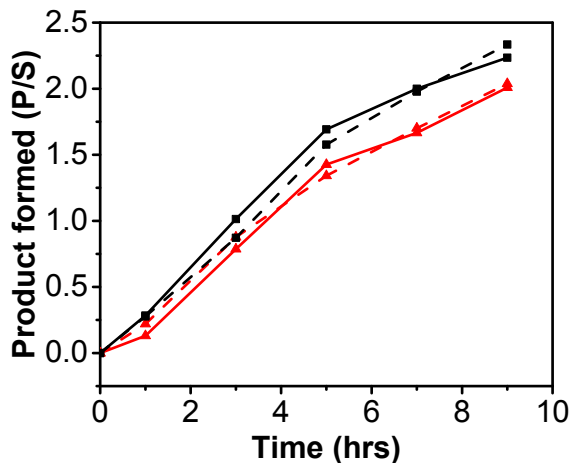
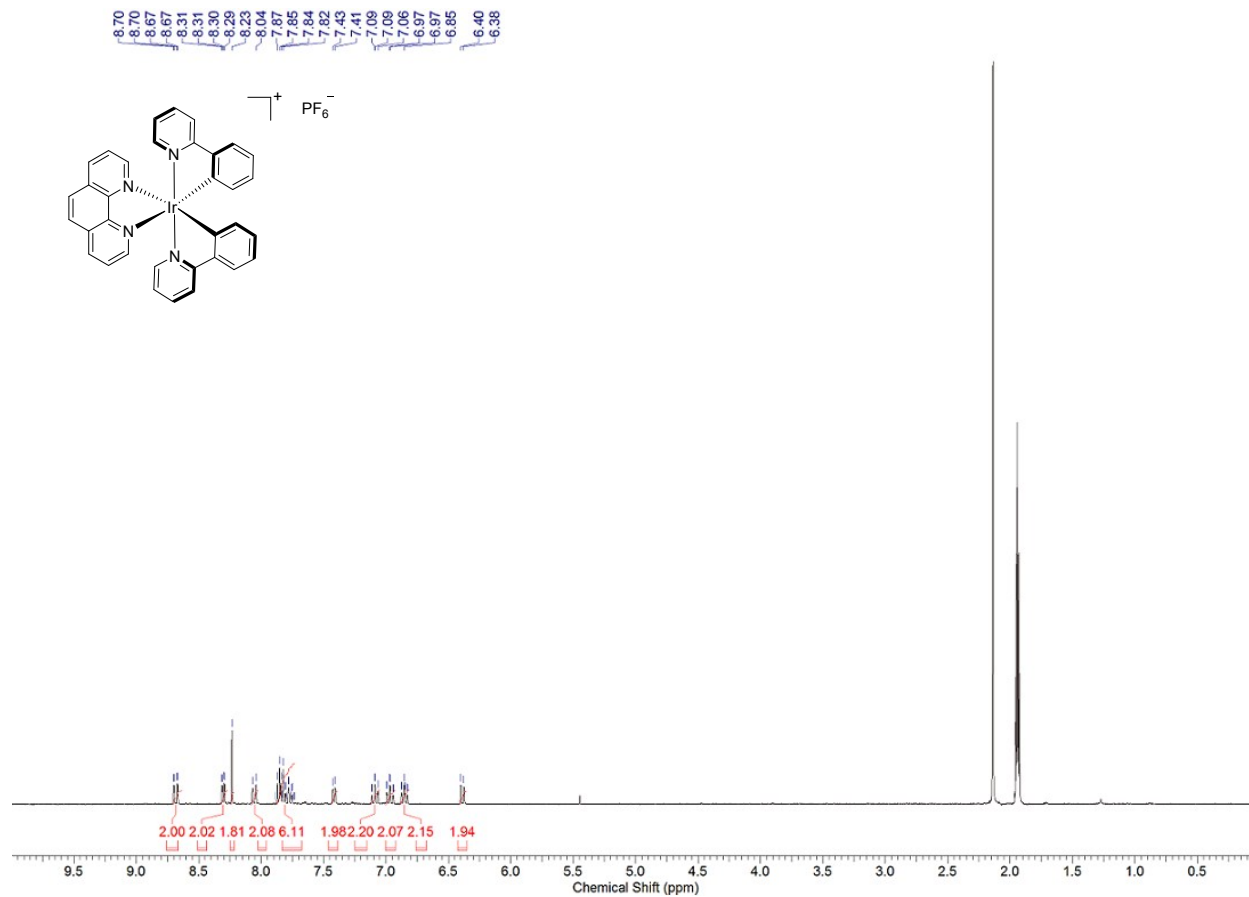


**Fig. S11** Formation of trifluoromethylated quinoline followed using photocatalyst **1** (■) and photocatalyst **4** (▲) with a  $\text{CF}_3\text{SO}_2\text{Cl}$  concentration of 0.22 M (solid lines) and 1.10 M (dashed lines). The product formed was quantified by taking the total integrated area for all product peaks, P, divided by the total integrated area for the internal standard, S, (cyclohexane carbonitrile) in the GC-MS traces.

## 12. NMR Spectra

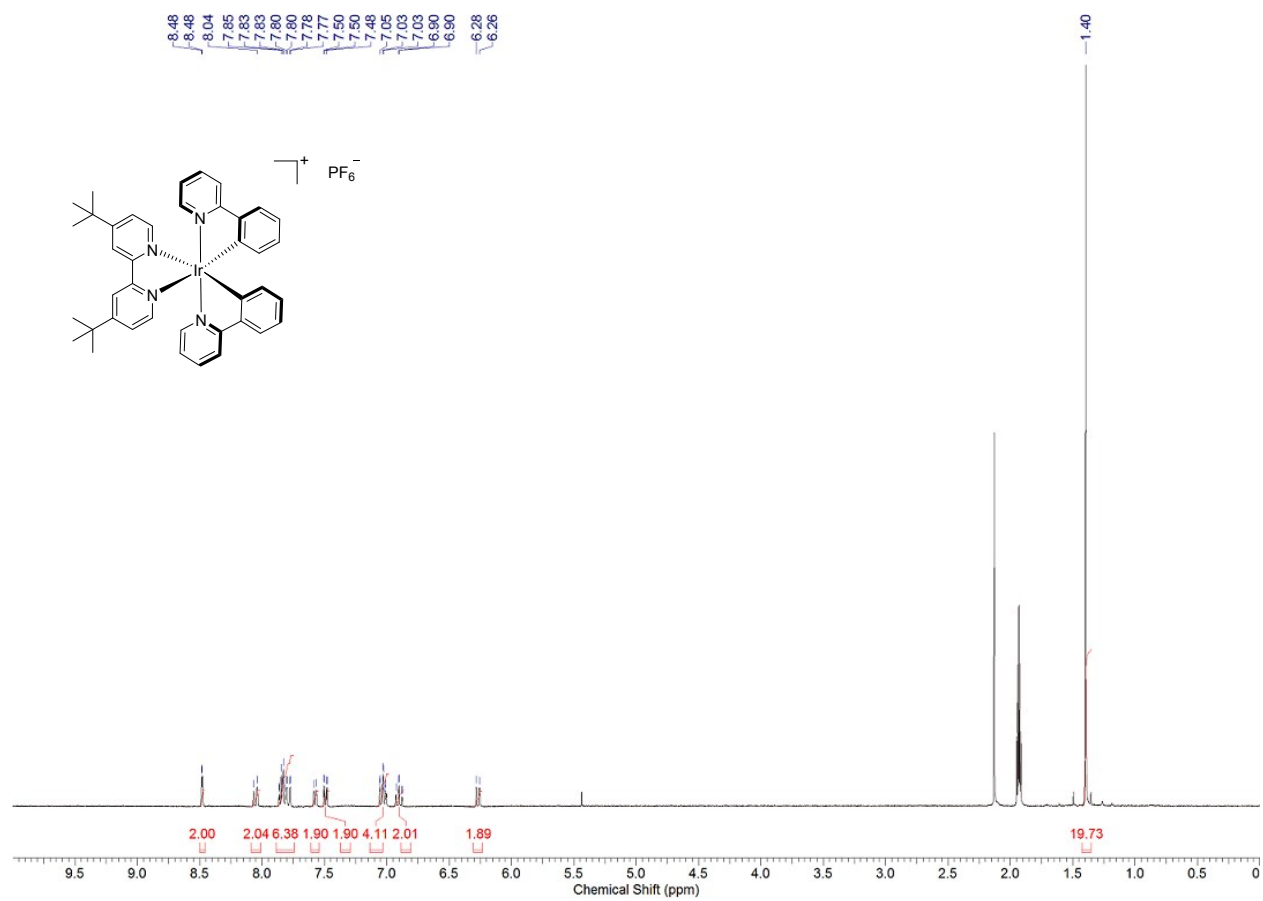
[Ir(ppy)<sub>2</sub>phen][PF<sub>6</sub>] (1):

<sup>1</sup>H NMR, 300 MHz, CD<sub>3</sub>CN:



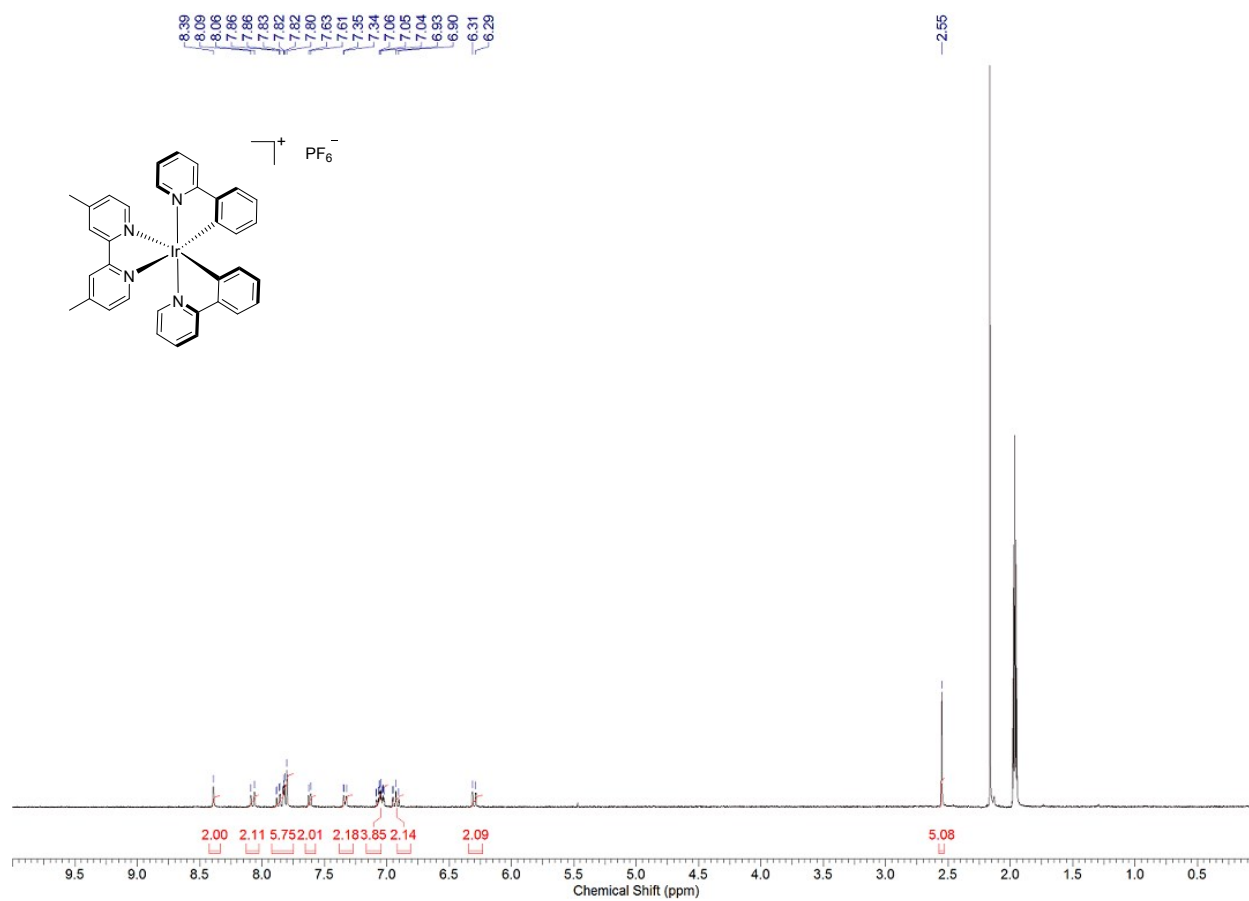
**[Ir(ppy)<sub>2</sub>dtbbpy][PF<sub>6</sub>] (2):**

**<sup>1</sup>H NMR, 300 MHz, CD<sub>3</sub>CN:**



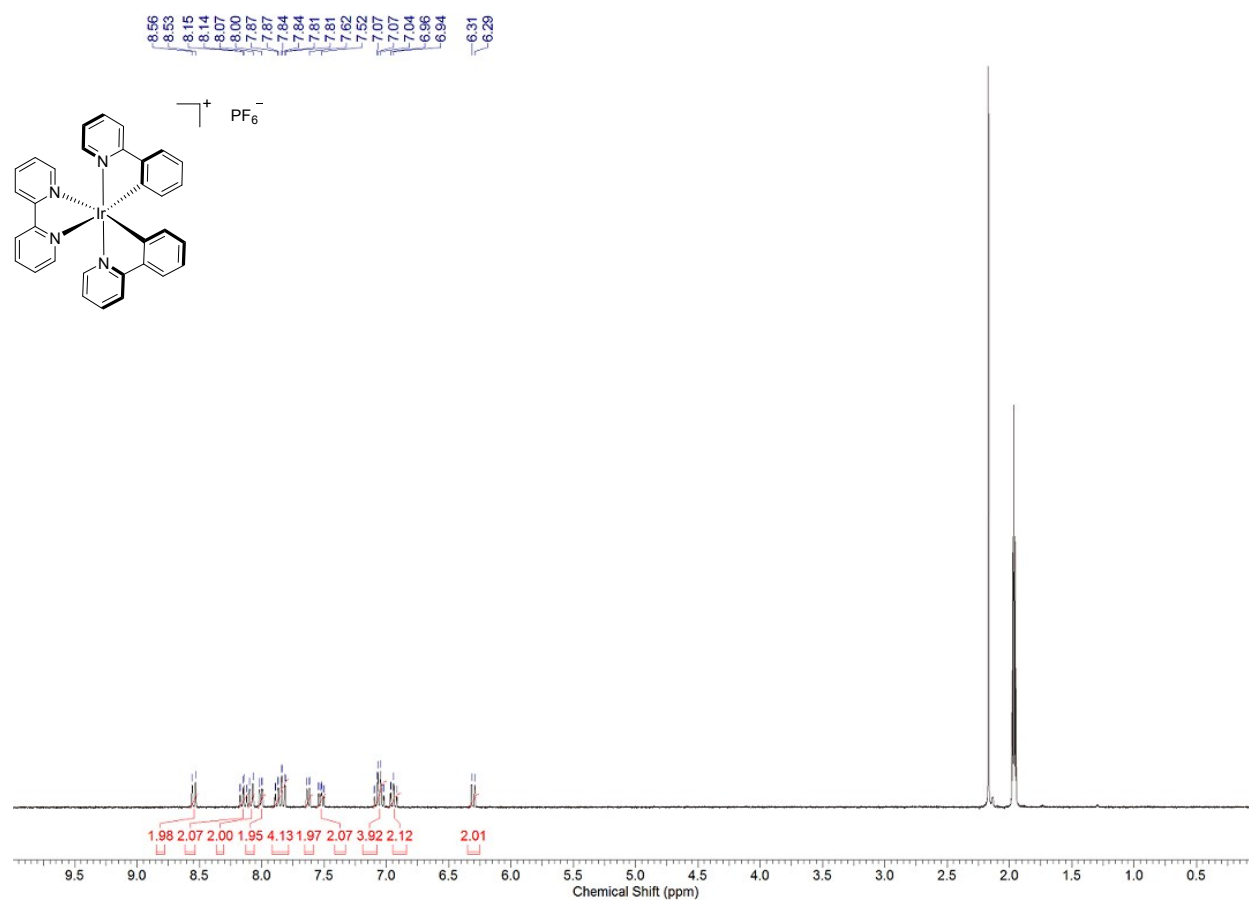
[Ir(ppy)<sub>2</sub>dmbpy][PF<sub>6</sub>] (3):

<sup>1</sup>H NMR, 300 MHz, CD<sub>3</sub>CN:



**[Ir(ppy)<sub>2</sub>bpy][PF<sub>6</sub>] (4):**

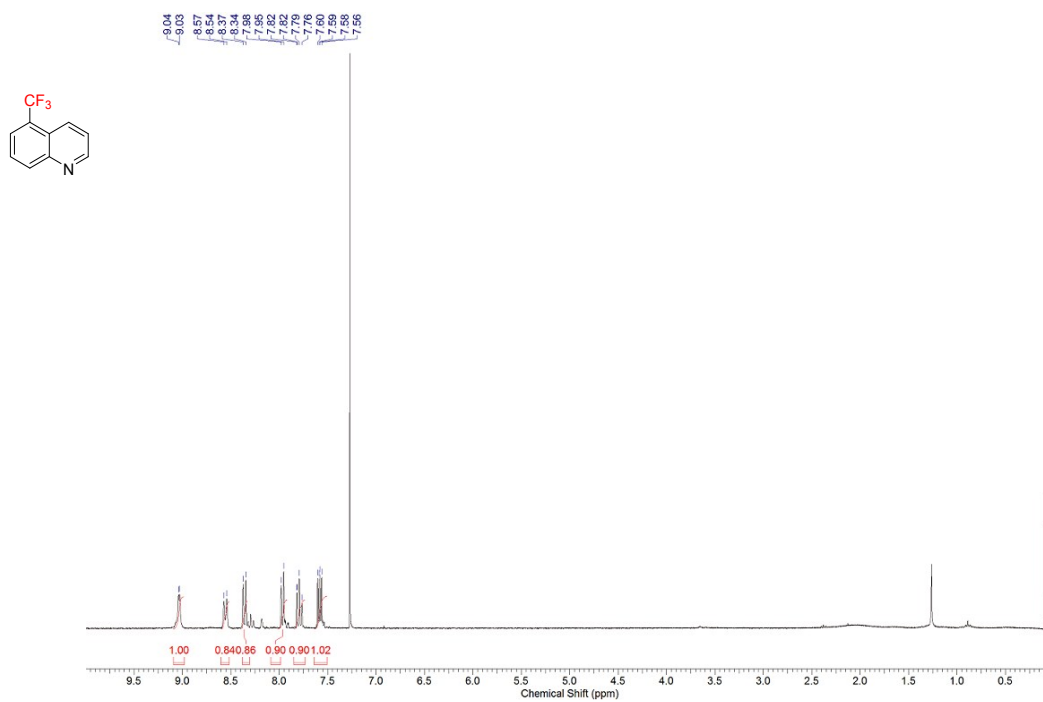
**<sup>1</sup>H NMR, 300 MHz, CD<sub>3</sub>CN:**



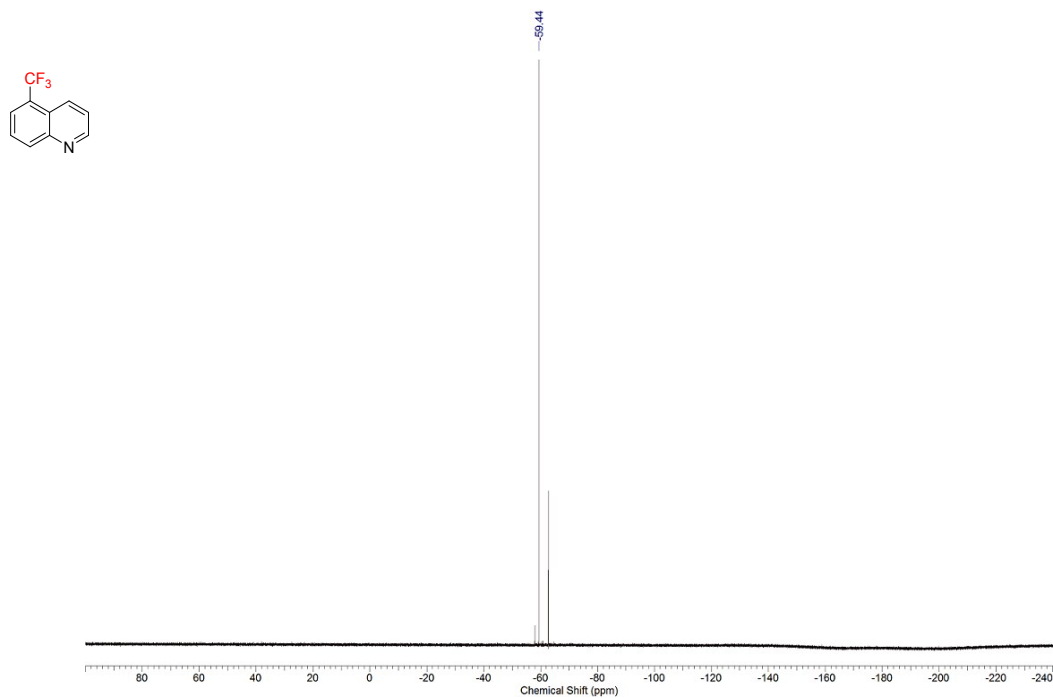


5-trifluoromethylquinoline:

$^1\text{H}$  NMR, 300 MHz,  $\text{CDCl}_3$ :

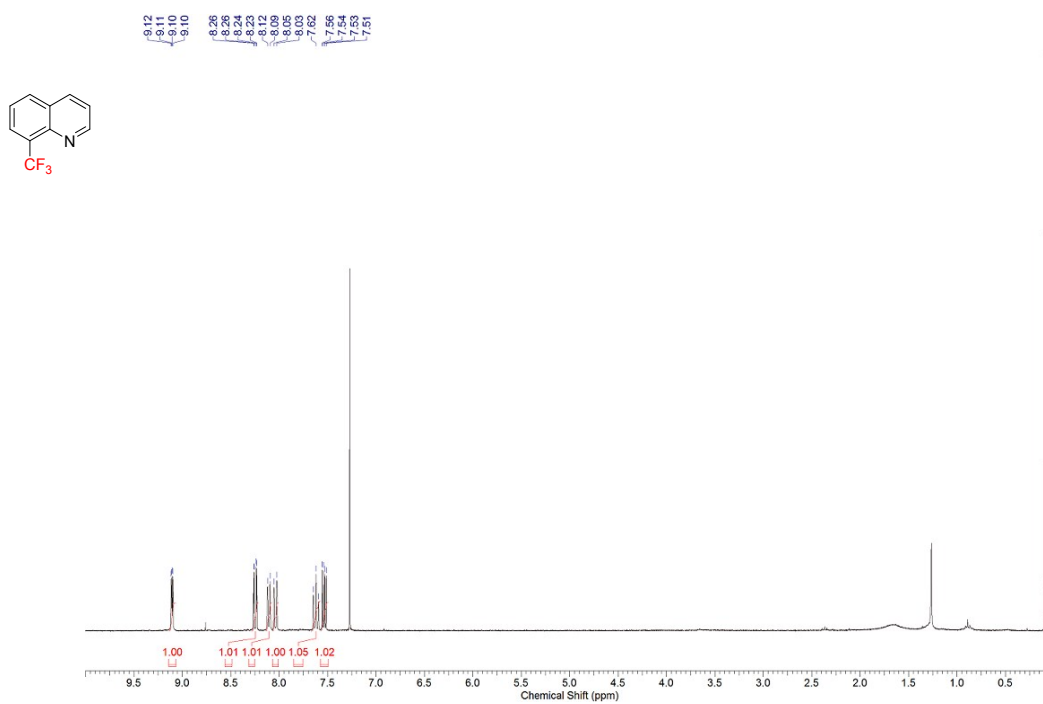


$^{19}\text{F}$  NMR, 282 MHz,  $\text{CDCl}_3$ :

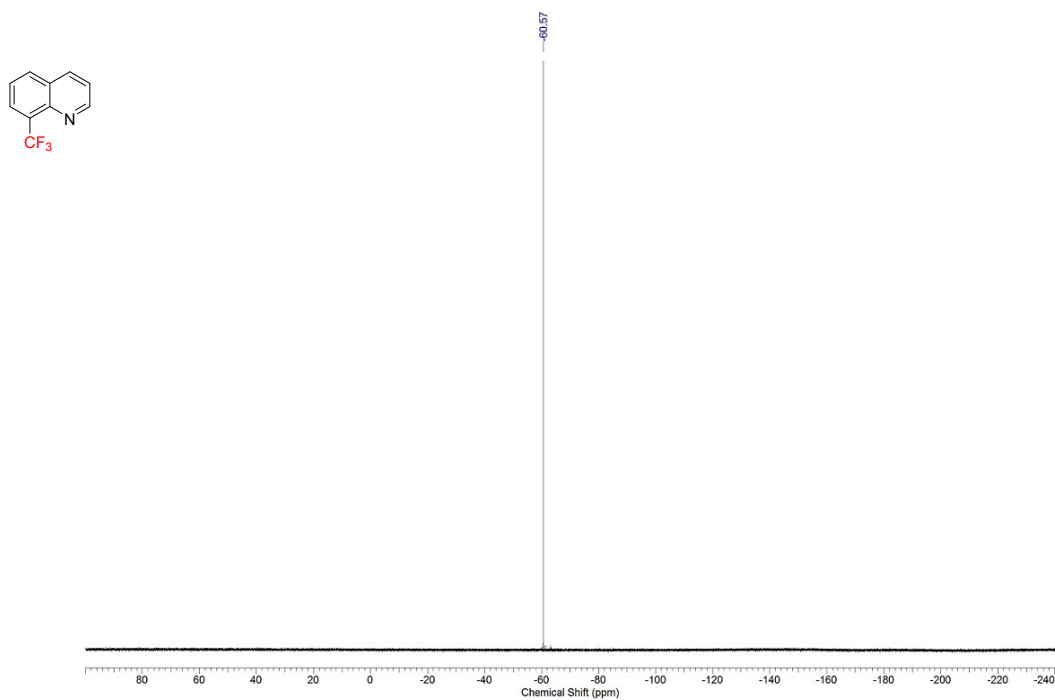


8-trifluoromethylquinoline:

<sup>1</sup>H NMR, 300 MHz, CDCl<sub>3</sub>:

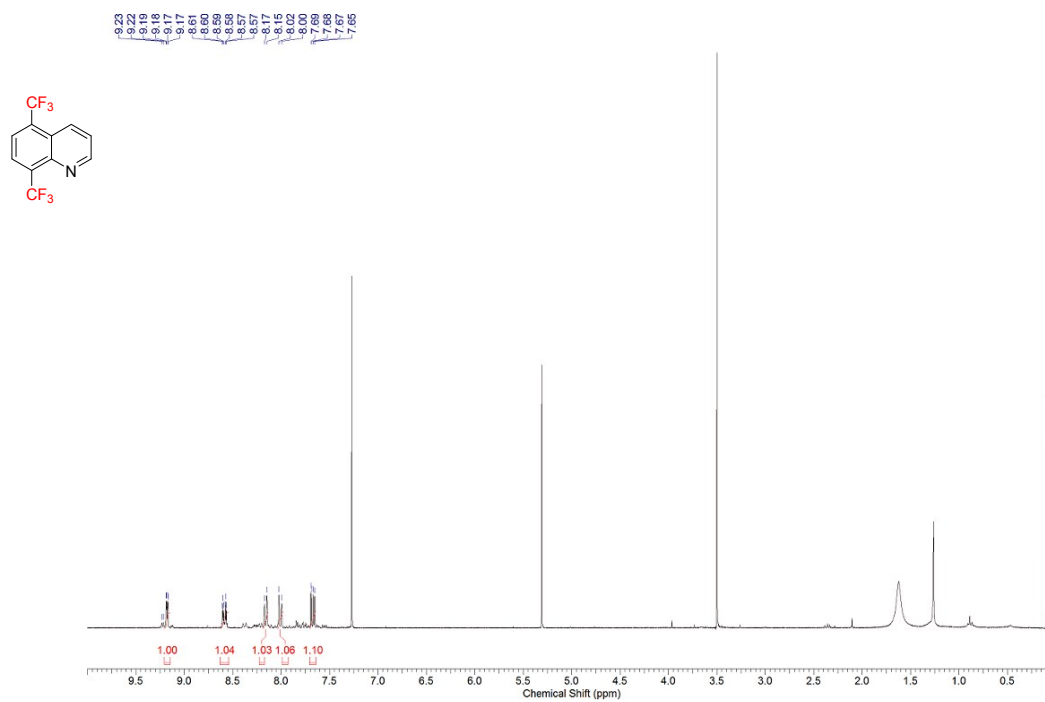


<sup>19</sup>F NMR, 282 MHz, CDCl<sub>3</sub>:

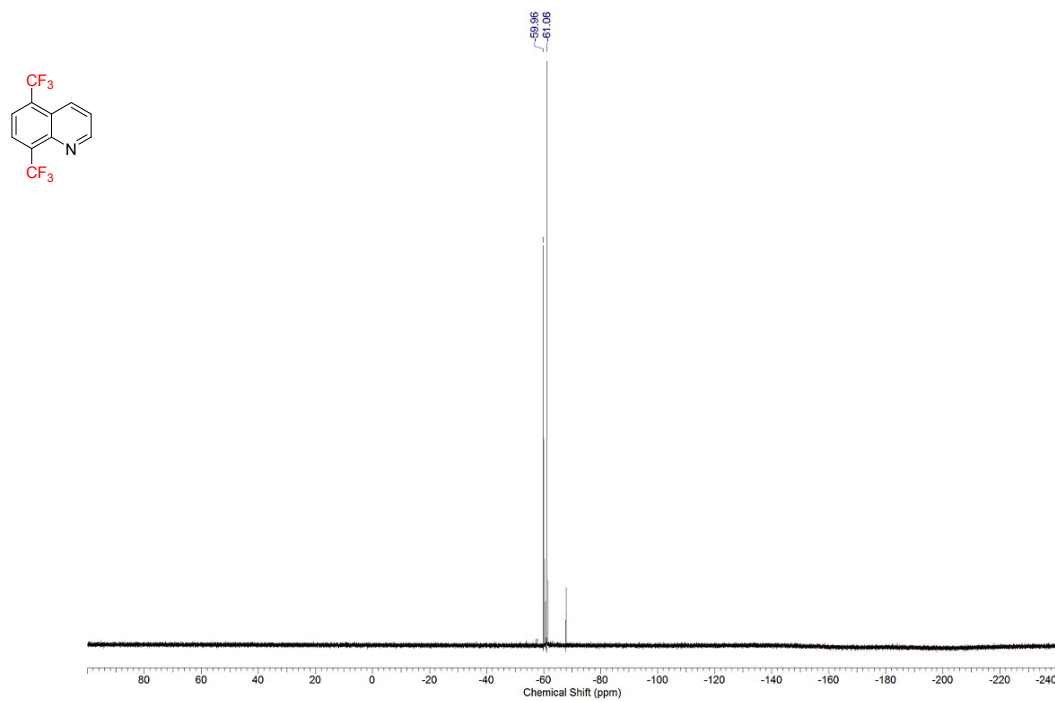


5,8-ditrifluoromethylquinoline:

<sup>1</sup>H NMR, 300 MHz, CDCl<sub>3</sub>:



<sup>19</sup>F NMR, 282 MHz, CDCl<sub>3</sub>:



### 13. References

- 1 A. J. Howarth, D. L. Davies, F. Leij, M. O. Wolf, B. O. Patrick, *Dalton Trans.*, 2012, **41**, 10150.
- 2 (a) M. S. Lowry, W. R. Hudson, Jr. R. A. Pascal, S. Bernhard, *J. Am. Chem. Soc.*, 2004, **126**, 14129; (b) J. D. Slinker, A. A. Gorodetsky, M. S. Lowry, J. Wang, S. Parker, R. Rohl, S. Bernhard, G. G. Malliaras, *J. Am. Chem. Soc.*, 2004, **126**, 2763; (c) K. P. S. Zanoni, B. K. Kariyazaki, A. Ito, M. K. Brennaman, T. J. Meyer, N. Y. M. Iha, *Inorg. Chem.*, 2014, **53**, 4089; (d) S. Ladouceur, D. Fortin, E. Zysman-Colman, *Inorg. Chem.*, 2011, **50**, 11514.
- 3 D. A. Nagib, D. W. C. MacMillan, *Nature*, 2011, **480**, 224.
- 4 (a) *JP. Pat.*, JP 2008115105 A, 2008; (b) G. Danoun, B. Bayarmagnai, M. F. Grünberg, L. J. Gooßen, *Angew. Chem. Int. Ed.*, 2013, **52**, 7972.
- 5 IUPAC Goldbook. Gibbs Energy of Photoinduced Electron Transfer. <http://goldbook.iupac.org/GT07388.html> (accessed Apr 7, 2016).